

Reprinted from

JAPANESE JOURNAL OF
**APPLIED
PHYSICS**

REGULAR PAPER

**Improvement of Surge Protection by Using an AlGa_N/Ga_N-Based
Metal–Semiconductor–Metal Two-Dimensional Electron Gas Varactor**

Yi-Cherng Ferng, Liann-Be Chang, Atanu Das, Ching-Chi Lin, Chun-Yu Cheng, Ping-Yu Kuei, and Lee Chow

Jpn. J. Appl. Phys. **51** (2012) 124201

Improvement of Surge Protection by Using an AlGa_N/Ga_N-Based Metal–Semiconductor–Metal Two-Dimensional Electron Gas Varactor

Yi-Cherng Ferng¹, Liann-Be Chang^{2*}, Atanu Das¹, Ching-Chi Lin¹, Chun-Yu Cheng¹, Ping-Yu Kuei³, and Lee Chow⁴

¹Department of Electronic Engineering, Chang Gung University, Taoyuan 333, Taiwan

²Green Research Technology Center, Chang Gung University, Taoyuan 333, Taiwan

³Department of Electrical and Electronic Engineering, Chung Cheng Institute of Technology, National Defense University, Taoyuan 335, Taiwan

⁴Department of Physics, University of Central Florida, Orlando, FL 32816, U.S.A.

Received June 2, 2012; accepted October 15, 2012; published online November 26, 2012

In this paper, a varactor with metal–semiconductor–metal diodes on top of the (NH₄)₂S/P₂S₅-treated AlGa_N/Ga_N two-dimensional electron gas epitaxial structure (MSM-2DEG) is proposed to the surge protection for the first time. The sulfur-treated MSM-2DEG varactor properties, including current–voltage (*I*–*V*), capacitance–voltage (*C*–*V*), and frequency response of the proposed surge protection circuit, are presented. To verify its capability of surge protection, we replace the metal oxide varistor (MOV) and resistor (R) in a state-of-the-art surge protection circuit with the sulfur-treated MSM-2DEG varactor under the application conditions of system-level surge tests. The measured results show that the proposed surge protection circuit, consisted of a gas discharge arrester (GDA) and a sulfur-treated MSM-2DEG varactor, can suppress an electromagnetic pulse (EMP) voltage of 4000 to 360 V, a reduction of 91%, whereas suppression is to 1780 V, a reduction of 55%, when using only a GDA.

© 2012 The Japan Society of Applied Physics

1. Introduction

For protecting electronic systems against the natural or man-made surge threats, including lightning, electromagnetic pulse (EMP), electrostatic discharge (ESD), and so forth, nonlinear protection components such as gas discharge arrester (GDA), metal oxide varistor (MOV), and transient voltage suppressor (TVS) diodes are the state-of-the-art surge protection countermeasures.^{1–5} However, in these reported articles, the authors also mentioned that the shorter the rise time of a pulse, the higher is the needed voltage to fire the GDA that resulted in no significant voltage reduction in fast introduced surges. Although the MOV is with the high electrical nonlinearity, further work is required to address the various issues including its energy-rating limits and the difficulty of controlling its grain boundaries. Besides, there is a tradeoff between the surge protection capability and the parasitic capacitance effect in the MOV selection. The higher the surge protection capability of the MOV, the higher is the parasitic capacitance effect, resulting in a high insertion loss in the high frequency applications. Even though the TVS diodes are frequently used in the EMP protection circuits as fine protection device in combination with the GDA or MOV, standing the high-voltage pulses only for a limited time and having the parasitic capacitance are their problems. Therefore, it still draws much attention to find solutions^{6,7} in high frequency application and fast rising pulse surge protection.

With the good material properties and the rapid progress in growth and device processing, an AlGa_N/Ga_N high-electron mobility transistor (HEMT) is very promising for the high power applications.^{8–10} Furthermore, several studies have been extended to an AlGa_N/Ga_N varactor which is verified with a good capacitance swing^{11–13} and can be used for low-loss high-power RF switching.¹⁴ These merits show the potential qualities necessary for use in surge protection. In this paper, a varactor with metal–semiconductor–metal diodes on top of the (NH₄)₂S/P₂S₅-treated AlGa_N/Ga_N two-dimensional electron gas epitaxial structure (MSM-2DEG) is proposed to be employed as a series

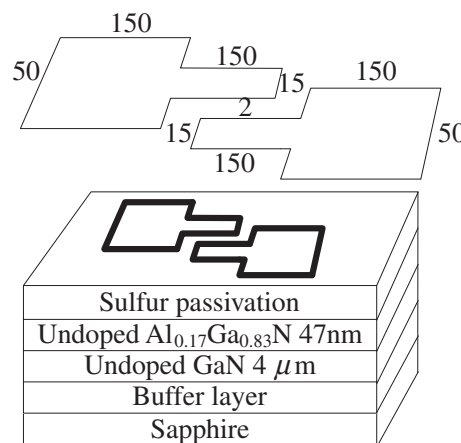


Fig. 1. Top view and cross-section of the sulfur-treated AlGa_N/Ga_N MSM-2DEG varactor.

surge blocker in association with a parallel GDA for the surge protection for the first time. Based on impedance formula $Z_c = 1/j\omega c$, under a normal operation the varactor behaves like a capacitor of relatively large capacitance (8.39 pF) for passing the signal, whereas under a higher voltage it acts as a much smaller capacitor (0.32 pF) for insulating the device from the line in the event of a surge and activating the GDA rapidly to discharge the excess surge energy. The DC electrical properties of the sulfur-treated varactor and the frequency response of the proposed surge protection circuit are presented. Furthermore, both EMP surge injection experiments and hysteresis characteristic measurements of the proposed surge protection circuit are conducted to investigate the surge protection capability and the surge reliability.

2. Experimental Procedure

Figure 1 shows the top view and cross-section of the (NH₄)₂S/P₂S₅-treated AlGa_N/Ga_N MSM-2DEG varactor with 9750 μm² electrode area in this study. An Al_{0.17}Ga_{0.83}N/Ga_N heterostructure was grown by metal–organic chemical vapor deposition (MOCVD) on a sapphire substrate. The AlGa_N/Ga_N heterostructures were treated with a

*E-mail address: liann@mail.cgu.edu.tw

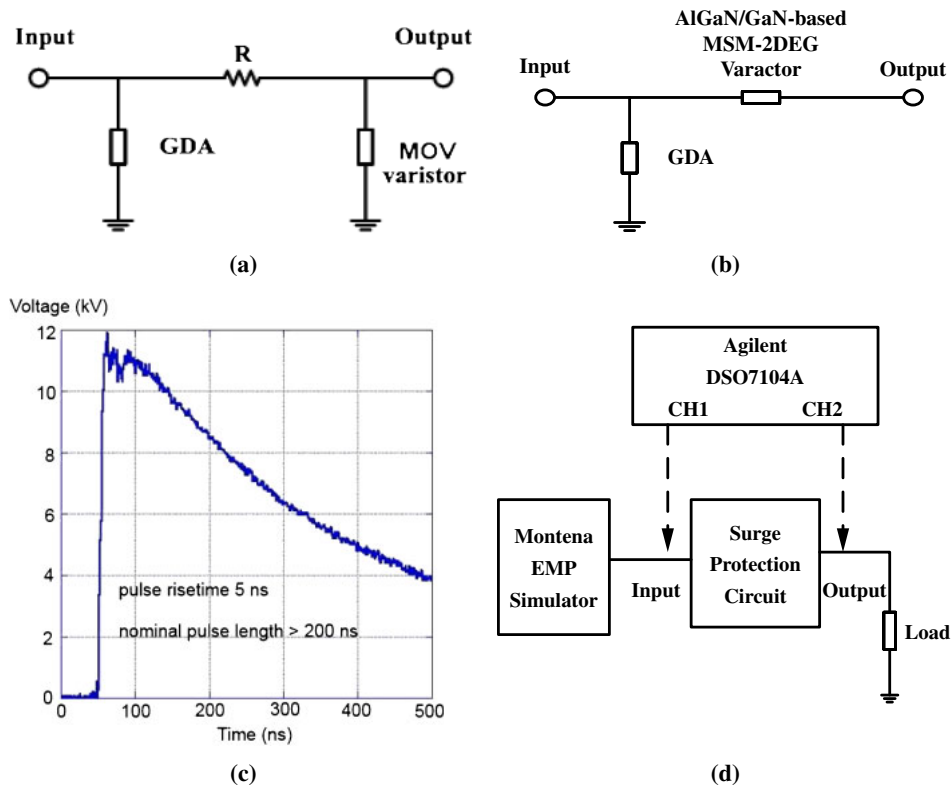


Fig. 2. (Color online) Schematic diagrams of (a) the state-of-the-art surge protection circuit,⁵⁾ (b) the proposed surge protection circuit, (c) a curve showing the applied EMP surge voltage, and (d) the testing configuration of the EMP surge injection experiments and hysteresis characteristic measurements with a 50 Ω loading.

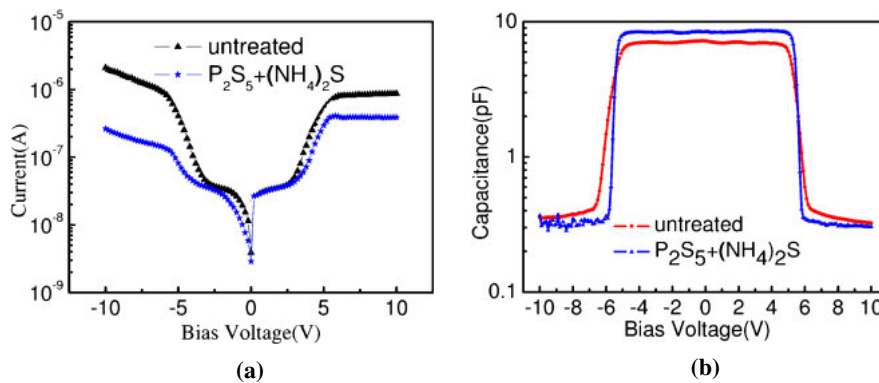


Fig. 3. (Color online) Measured (a) I - V curves and (b) C - V curves of the untreated and sulfur-treated AlGaIn/GaN MSM-2DEG varactors.

$(\text{NH}_4)_2\text{S}/\text{P}_2\text{S}_5$ solution for sulfur passivation prior to the Ni/Au metallization. More details can be found in our previous report.¹⁵⁾ The DC properties, including current–voltage (I - V) and capacitance–voltage (C - V), were measured by using a Keithley 2430 pulse mode source meter and an HP 4285A precision LCR meter, respectively. In addition, the frequency response was taken by an Agilent E8362C network analyzer. Furthermore, in the EMP surge injection experiments, the components of either the state-of-the-art or the proposed surge protection circuit, as shown in Figs. 2(a) and 2(b), were selected from a 90 V GDA, a 2 Ω resistor (R), a 50 pF ZnO varistor, and an 8.39 pF sulfur-treated AlGaIn/GaN MSM-2DEG varactor. Moreover, for a worst case study referring to the previous report,¹⁶⁾ both the EMP surge injection experiments and hysteresis characteristic measurements were conducted by a Montena EMP simulator,

generating an electromagnetic pulse surge voltage with a double-exponential waveform of 4–10 kV amplitude, a rise time of 5 ns, and a nominal pulse length greater than 200 ns, as shown in Fig. 2(c), for evaluating the surge protection capability and the surge reliability of the proposed surge protection circuit. The response signals were detected by an Agilent DSO7104A oscilloscope, as shown in Fig. 2(d).

3. Results and Discussion

The DC properties of untreated and $(\text{NH}_4)_2\text{S}/\text{P}_2\text{S}_5$ -treated AlGaIn/GaN MSM-2DEG varactors are presented in Fig. 3. As shown in Fig. 3(a), because the MSM-2DEG varactor consists of two Schottky diodes connected back-to-back above a 2DEG layer structure, the forward current and the reverse current are in similar trend.¹²⁾ Since the main current of Schottky diode is dominated by reversed bias, when the

reversed bias increases, a leakage current path occurs from reverse-bias depletion zone to forward-bias depletion zone. When the reversed bias further increases above the transition voltage (V_t), about ± 6 V in this study, the reverse-bias depletion zone penetrates through the 2DEG channel and causes an additional leakage current path, occurred from 2DEG channel to forward-bias depletion zone. This depletion of the 2DEG causes an increase of the channel resistance below this electrode. The reverse current saturates and becomes almost voltage independent,¹⁷⁾ the same as shown in Marso *et al.* report.¹²⁾ As shown in Fig. 3(b), when the reversed bias increases, the reverse-bias depletion zone increases, meanwhile the forward-bias depletion zone decreases. The serial equivalent capacitance is almost the same as that at the zero reversed bias. However, when the reversed bias further increases above the transition voltage (V_t), the reverse-bias depletion zone penetrates through the 2DEG channel and causes an additional 2DEG capacitance with a comparable low value. And then the serial equivalent capacitance is dominated by the relative low value 2DEG capacitance. Due to the $(\text{NH}_4)_2\text{S}/\text{P}_2\text{S}_5$ -treated case has a better surface state by reducing the native oxide and increasing the extra stable phosphorus compounds and sulfide on the grown surface, as demonstrated in our previous study,¹⁵⁾ the improvement of nonlinear behaviors, including the improved leakage current and the enlarged capacitance swing, are obtained. Furthermore, an improved Schottky barrier height (0.66 eV) of $(\text{NH}_4)_2\text{S}/\text{P}_2\text{S}_5$ -treated sample, by calculating from the measured I - V curves and using the thermionic emission model,¹⁸⁾ is obtained as compared to that (0.65 eV) of the untreated sample. This also validates that the forming layer not only blocks the leakage current but also enhances the barrier height. Thus, the more robust sulfur-treated MSM-2DEG varactor is selected to be a surge blocker in the proposed surge protection circuit.

Figure 4 illustrates frequency response (S_{21}) of the proposed surge protection circuit, serving as a band-pass filter with a 3 dB bandwidth from 1.05 to 1.75 GHz. It reveals that the proposed surge protection circuit can be applied with the lower insertion loss in the high frequency (GHz), because of the sulfur-treated varactor staying in a relative low impedance in the normal operation for passing the signal with a relative low insertion loss, than that of the low frequency (MHz) surge protection circuit.⁵⁾ Meanwhile, because the low frequency response (S_{21}) was exhibited under 300 MHz, thus, the effective surge energy of the well-known high altitude nuclear electromagnetic pulse (HEMP) indicated under 100 MHz¹⁾ can be suppressed to prevent electronic systems from damage.

In the EMP surge injection experiments, the resulted residual EMP surge voltages of the surge protection circuits were summarized as shown in Fig. 5(a). The measured results show that the proposed surge protection circuit has better surge protection capability than that of the state-of-the-art surge protection circuit,⁵⁾ as shown in Fig. 2(a), and the surge protection circuit with GDA only. This is demonstrated in Fig. 5(b). The response time of the response current, response current, and residual EMP surge voltage detected on the sulfur-treated MSM-2DEG varactor as shown in Fig. 2(b) are 50, 34, and 34% respectively of that detected on the MOV as shown in Fig. 2(a). It means that the

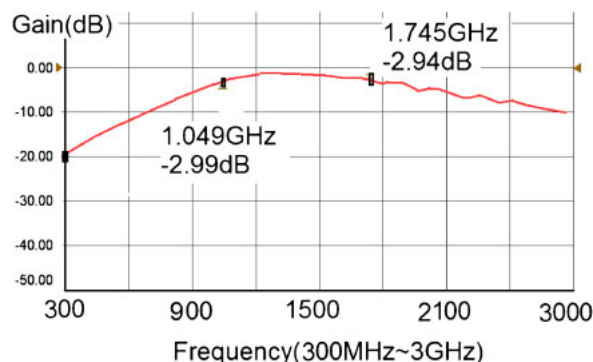
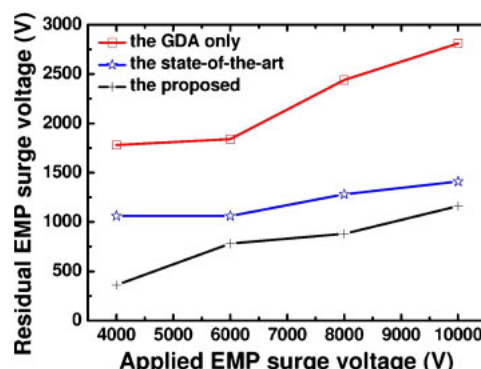
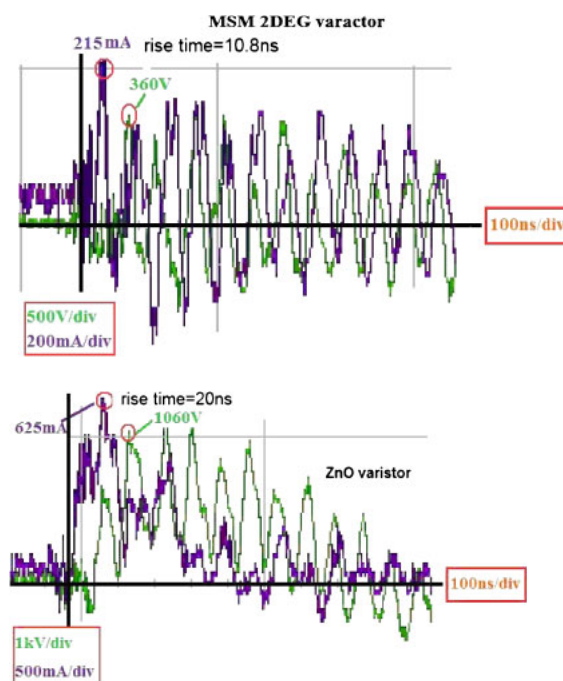


Fig. 4. (Color online) Measured frequency response (S_{21}) of the proposed surge protection circuit, serving as a band-pass filter.



(a)



(b)

Fig. 5. (Color online) (a) Residual EMP surge voltage of the GDA only, the state-of-the-art,⁵⁾ and the proposed surge protection circuits. (b) Response time of response current, response current, and residual EMP surge voltage detected on sulfur-treated MSM-2DEG varactor, as shown in Fig. 2(b), and ZnO varistor, as shown in Fig. 2(a), respectively under a 4000 V EMP surge voltage.

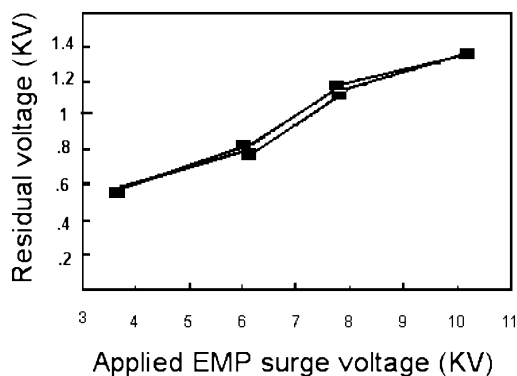


Fig. 6. Hysteresis characteristic measurements of the proposed surge protection circuit.

rapid response time of the sulfur-treated MSM-2DEG varactor is the critical factor of the resulted surge protection capability. Namely, the sulfur-treated MSM-2DEG varactor can act as a resistor in the state-of-the-art surge protection circuit⁵⁾ for blocking the surge energy and for rapidly activating the GDA for quickly bypassing the most surge energy.

The hysteresis characteristic of the residual EMP surge voltage of the proposed surge protection circuit was shown in Fig. 6. It reveals good surge reliability on the proposed surge protection circuit and the sulfur-treated MSM-2DEG varactor due to the small variances of the residual EMP surge voltage and the functional work of the protective device through the entire measurements.

4. Conclusions

In this paper, a sulfur-treated AlGaIn/GaN MSM-2DEG varactor, acting as a prompt surge stopper and as a faster trigger for the GDA, has been demonstrated for good surge protection. Under a 4000 V EMP surge voltage, due to the MSM-2DEG varactor having a prompt response time, thus, the proposed surge protection circuit exhibits a better surge suppression of 91% than that of 73% in the state-of-the-art surge protection circuit,⁵⁾ even though the MSM-2DEG varactor has a relative low capacitance. Besides, the frequency response of the proposed surge protection circuit also

shows the potential application in the high frequency (GHz). Furthermore, due to the MSM-2DEG varactor having a fully compatible manufacturing process with HEMT,¹¹⁾ hence, it can be a good candidate for providing a promising surge protection capability that may open up the on-chip surge protection for future high power HEMT applications.¹⁹⁾

Acknowledgements

The authors would like to thank the Green Technology Research Center of Chang Gung University and the National Science Council for their support of this study.

- 1) T. Weber, R. Krzikalla, and J. L. ter Haseborg: *IEEE Trans. Electromagn. Compat.* **46** (2004) 423.
- 2) K. K. Jha: Proc. 9th Int. Conf. Electromagnetic Interference and Compatibility, 2006, p. 389.
- 3) J. Ribič, J. Pihler, and J. Voršič: *IEEE Trans. Power Deliv.* **22** (2007) 2199.
- 4) A. Haddad, D. M. German, R. T. Waters, and Z. Abdul-Malek: *IEE Proc.—Gener. Transm. Distrib.* **148** (2001) 21.
- 5) *IEEE Standard C62.42* (2005).
- 6) B. J. Kim, Y. W. Lee, S. Y. Choi, S. J. Yun, and H. T. Kim: *IEEE Electron Device Lett.* **31** (2010) 14.
- 7) S. H. Dai, J. J. Peng, C. C. Chen, C. J. Lin, and Y. C. King: *Jpn. J. Appl. Phys.* **49** (2010) 04DP13.
- 8) S. Keller, Y. F. Wu, G. Parish, N. Ziang, J. J. Xu, B. P. Keller, S. P. DenBaars, and U. K. Mishra: *IEEE Trans. Electron Devices* **48** (2001) 552.
- 9) Y. F. Wu, A. Saxler, M. Moore, R. P. Smith, S. Sheppard, P. M. Chavarkar, T. Wisleder, U. K. Mishra, and P. Parikh: *IEEE Electron Device Lett.* **25** (2004) 117.
- 10) I. P. Smorchkova, M. Wojtowicz, R. Sandhu, R. Tsai, M. Barsky, C. Namba, P. S. Liu, R. Dia, M. Truong, D. Ko, J. Wang, H. Wang, and A. Khan: *IEEE Trans. Microwave Theory Tech.* **51** (2003) 665.
- 11) M. Marso, M. Wolter, P. Javorka, A. Fox, and P. Kordoš: *Electron. Lett.* **37** (2001) 1476.
- 12) M. Marso, A. Fox, G. Heidelberger, P. Kordoš, and H. Lüth: *IEEE Electron Device Lett.* **27** (2006) 945.
- 13) C. S. Chu, Y. Zhou, K. J. Chen, and K. M. Lau: *IEEE Electron Device Lett.* **26** (2005) 432.
- 14) G. Simin, A. Koudymov, Z. J. Yang, V. Adivarahan, J. Yang, and M. A. Khan: *IEEE Electron Device Lett.* **26** (2005) 56.
- 15) Y. C. Ferng, L. B. Chang, A. Das, C. Y. Chen, and C. C. Lin: *Electrochem. Solid-State Lett.* **13** (2010) H350.
- 16) J. F. Xu, W. Y. Yin, J. F. Mao, and L. W. J. Li: *IEEE Trans. Electromagn. Compat.* **50** (2008) 340.
- 17) M. Marso, M. Horstmann, H. Hardtdegen, P. Kordoš, and H. Lüth: *Solid-State Electron.* **41** (1997) 25.
- 18) V. Aubry and F. Meyer: *J. Appl. Phys.* **76** (1994) 7973.
- 19) J. Kuzmík, D. Pogany, E. Gornik, P. Javorka, and P. Kordoš: *Appl. Phys. Lett.* **83** (2003) 4655.